Available online at www.sciencedirect.com

SciVerse ScienceDirect

Energy Procedia 00 (2017) 000–000

Energy Procedia

www.elsevier.com/locate/procedia

IV International Seminar on ORC Power Systems, ORC2017
13-15 September 2017, Milano, Italy

Towards the Validation of a CFD Solver for Non-ideal Compressible Flows

A. J. Head[a,*], S. Iyer[a], C. de Servi[a,b], M. Pini[a]

[a] *Propulsion & Power*
Aerospace Engineering
Delft University of Technology
Kluyverweg 1, 2629 HS Delft, The Netherlands
[b] *VITO, Boeretang 200, Mol 2400, Belgium*

Abstract

Mini ORC power systems with the capability to deliver 3-50 kWe are receiving increased recognition for applications such as heat recovery from automotive engines, or distributed power generation from geothermal reservoirs and solar irradiation. Efficient and reliable expanders are the enabling components of such power systems, and all the related developments are currently at the research stage [1]. In the open literature experimental gas dynamic data is limited concerning the fluids and the flow conditions of interest for ORC expanders [2]. Therefore, CFD tools used for the fluid dynamic design of these components cannot be validated against reliable test cases. To bridge this gap, new experimental facilities are currently being built, such as the ORCHID set-up [3]. The availability of proper experimental datasets is not, however, the sole requirement for validating a CFD code. Another precondition, equivalently important, is to define an appropriate validation methodology. This paper introduces the first steps towards the validation of a CFD solver for non-ideal compressible flows. Notably, a numerical procedure based on uncertainty quantification analysis has been conceived to assess the accuracy of the thermophysical sub-model of the code, i.e. the equation of state (EoS). Due to the lack of suitable experimental data, a synthetic dataset is generated and used to investigate the validity of the procedure. The associated validation exercise confirms the applicability of the proposed procedure, but also points out that the adopted validation metrics should be complemented with additional statistical indicators.

Peer-review under responsibility of the scientific committee of the IV International Seminar on ORC Power Systems.

Keywords: Verification and Validation ; NICFD ; Uncertainty Quantification ; Design of Experiments

1. Introduction

Despite the large research efforts dedicated towards organic Rankine cycles (ORC) in the last decades, the aerodynamic design of ORC turbo-expanders still relies on CFD codes whose predictive capability is unknown. To the authors' knowledge, commercial and open source CFD tools such as Ansys CFX and SU2 [4] have been verified for a number of test cases regarding internal flow applications with dense organic fluids [5] but they have not been validated yet. The main reason is the unavailability of experimental gas-dynamic data in the open literature representative

* Corresponding author. T +31 (0)15 278 5293
E-mail address: a.j.head@tudelft.nl

Peer-review under responsibility of the scientific committee of the IV International Seminar on ORC Power Systems.

of the flow conditions typically encountered in ORC turbines, namely, in close proximity to the critical point, with strong non-ideal gas effects, and relatively high Mach numbers. To this purpose, dedicated experimental facilities are currently being built, such as the ORCHID set-up [3] and CLOWT [6], while the TROVA test rig [7] has recently become operative. These research efforts have resulted in the publication of the first measurements regarding a subcritical expansion in a pure organic vapour [8]. Extensive experimental campaigns specifically conceived for the purpose of validating non-ideal compressible fluid dynamics (NICFD) codes are then expected to be published in the near future.

The availability of proper experimental datasets is not, however, the sole requirement for a validation assessment. It is equally important to define an appropriate method on how to compare the model predictions and the measurements, and how to infer the reliability of the model from this comparison. The need for adopting a systematic Verification and Validation (V&V) methodology for code quality assurance is a topic well documented in the literature [9–12]. The American Institute for Aeronautics and Astronautics (AIAA) and the American Society of Mechanical Engineers (ASME) produced the first V&V guidelines in the area of CFD [13,14]. According to these references, validation is the process of determining by statistical means the degree of confidence with which a model is an accurate representation of the physical phenomena of interest in its domain of applicability. In other words, since models, by definition, as well as measurements are consistent with reality only with a given level of approximation, their comparison cannot be accomplished without first identifying and quantifying the uncertainty sources which affect both of them. The predictive capability of the model can then be assessed by statistical tests or appropriate metrics that take into account the uncertainty range associated to each single physical observation and the corresponding model calculation.

As estimating measurement and prediction uncertainty strongly depends on the characteristics of the experiments and the model, the adopted validation method has to be tailored somewhat to the problem at hand. The present work introduces the first steps towards the validation of a CFD solver for non-ideal compressible flows. Notably, a validation framework is developed to assess the accuracy of the thermophysical sub-model of the code, namely the equation of state (EoS). Due to the lack of suitable experimental data, a synthetic dataset is generated and used to demonstrate the validity of the procedure. The paper is structured as follows. Sect. 2 introduces the adopted validation approach and metrics. The validation test cases, namely the chosen experiments, are discussed in Sect. 3, while the simulation model and the uncertainty quantification (UQ) method used to estimate the uncertainty in the CFD code predictions is described in Sect. 4. Finally, the validation assessment is exemplified in Sect. 5.

2. Validation of a CFD Code for NICFD

The validation metrics adopted in this work to compare the experimental data and the model predictions are those first considered by Coleman [15] and Eca et al. [16]. The first one is the *validation standard uncertainty*,

$$U_{\mathrm{val}} = \sqrt{{U_{\mathrm{num}}}^2 + U_{\mathrm{input}}^2 + U_{\mathrm{D}}^2}; \tag{1}$$

where, U_{num} is the uncertainty in the model predictions, hereinafter termed as system response quantities (SRQ), due to the *numerical* procedure adopted to solve the equations, U_{input} is the uncertainty due to imperfect knowledge of code *inputs* (fluid properties, flow geometry and/or boundary conditions), and U_{D} is the uncertainty in the *experimental* results. The U_{num} includes three different components: the round-off, iterative and discretisation error. The first two error sources can be considered negligible if compared to the third one, provided that double precison values are used together with sufficiently converged solutions. Discretisation errors also become negligible with increasing grid-refinement [10] and procedures described by Celik [17] can be adopted to assess their relevance.

The second, is the *validation comparison error*

$$E = S - D; \tag{2}$$

where S is the numerical prediction and D is the experimental value of the considered SRQ. The goal of the procedure is to estimate the interval $[E - U_{\mathrm{val}}, E + U_{\mathrm{val}}]$ that contains the modelling error, δ_{model}, with a 95 % confidence level. The model needs to be improved if $|E| \gg U_{\mathrm{val}}$, however, if $|E| \leqslant U_{\mathrm{val}}$ then the model is capable of predicting the physics of the problem under investigation. The magnitude of $|E|$ relative to U_{val} is somewhat arbitrary and must be defined for each specific case study.

2.1. Computational Submodels

A CFD code can be decomposed into different computational sub-models. Considering the physical phenomena occurring in ORC turbines, there are three predominant sub-models to be validated: the turbulence, transport and

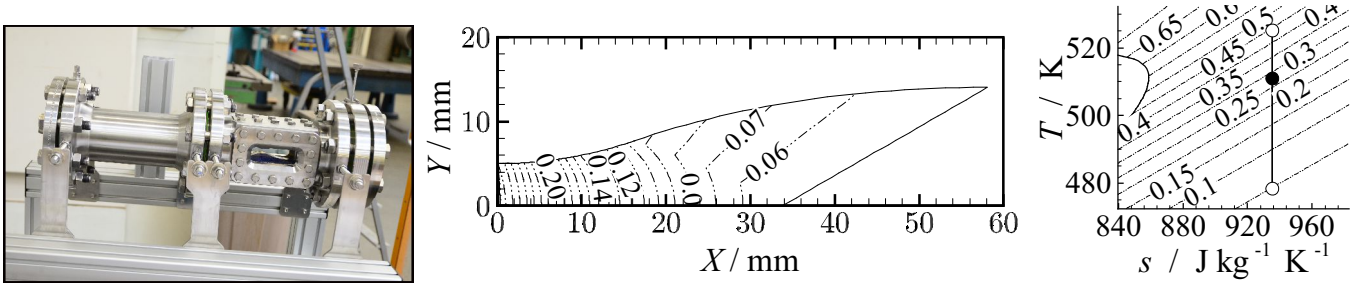

(a) (b) (c)

Fig. 1: a) The ORCHID Nozzle TS b) The nozzle profile created with the MoC: The top contains contours of 1-Z (-·-·-). c) *Ts* diagram showing the corresponding isentropic expansion with contours of 1-Z (-·-·-). ● indicates the nozzle throat and ○ indicates the inlet and outlet.

thermophysical model, i.e., the Equation of State (EoS) [11]. Each computational sub-model has *ad-hoc* or material dependent closure parameters, e.g., the critical point properties in the case of the EoS, which are affected by uncertainties.

When the system being modeled, as in the problem at hand, encompasses many interacting physical phenomena, the validation process is generally hierarchical: a validation test is performed for each subcomponent of the CFD code on the basis of relatively simpler experiments. It is apparent that for the objective of the present work, the first sub-model to be validated is thermophysical one, since it is impossible to define validation experiments for the turbulence and transport sub-models which do not require the use of an EoS for their simulation.

3. Envisaged Experiments

The first envisaged validation experiments aims at investigating shock wave patterns in a NICFD flow by means of the Schlieren technique. Shock waves can be generated by inserting models/obstacles of varying geometry – e.g., slender pins, and instrumented wedge or diamond shapes – within the diverging part of a de Laval nozzle [18]. The second experimental investigation consists in the measurement of the variation of static pressure during an expansion process, for instance by placing multiple pressure taps along the profile of the same de Laval nozzle used in the previous experiment.

These experimental campaigns will be conducted in the ORCHID set-up [3]. The Balance of Plant[1](BoP) of such an experimental facility closely integrates two different Test Sections (TS's) which can be alternatively fed and used, thus making the set-up *hybrid*. Fig 1a shows the first TS, a de Laval nozzle. The second TS is, instead, a test-bench for mini-ORC expanders. The nozzle TS is equipped with two optical access points in order to carry out optical measurements of the flow field. The design working fluid of the ORCHID is MM and the operating conditions for the nozzle TS are reported by Head et al. [3].

Figure 1b and 1c show the departure of the volumetric characteristics of siloxane MM from gas ideality $1 - Z$, where $Z = p(\rho RT)^{-1}$, along a possible expansion process in the ORCHID nozzle. As expected, the non-ideal effects are more pronounced at the initial part of the expansion ($Z_{\text{inlet}} \approx 0.55$), while at the exit section the fluid approaches the ideal gas behavior ($Z \approx 0.95$). Notice that, most likely, it will not be possible to generate shock waves close to the nozzle throat due to blocking effects induced by the inserted obstacle [19].

4. Uncertainty Quantification Framework

To validate the thermophysical sub-model, an uncertainty quantification (UQ) framework is required to calculate U_{input}. The numerical framework consists of two main steps. In the first one, a steady 2D inviscid solution of the flow-field in the nozzle (advection scheme second order accurate) is obtained using the Ansys CFX solver for a half-nozzle with symmetry conditions along the mid plane. Subsequently, the shock wave inclination is determined by first extracting the undisturbed static flow quantities, e.g., pressure, density, Mach number and velocity, at pre-

[1] The BoP consists of all infrastructural components of the set-up with the exception of the two TS's.

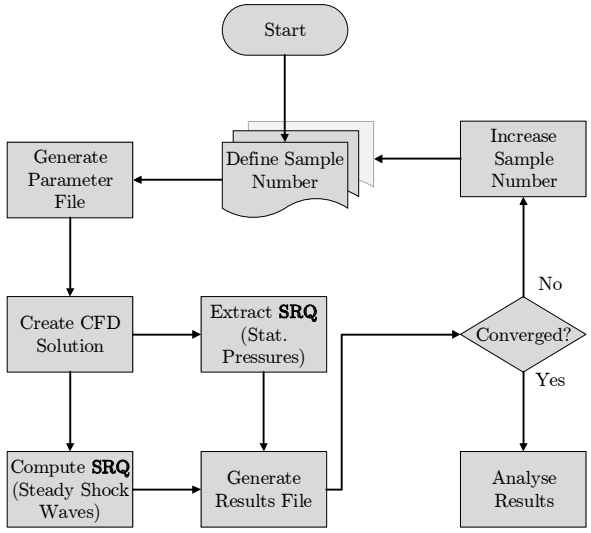

Fig. 2: Workflow of the Calculation Method

Table 1: MM Input Uncertainties

Parameter	Nominal	Uncertainty (%)
Comp. Sub-model		
T_c / °C *	245.60	±3 [22]
P_c / bar*	19.40	±5 [22]
ω [-]+	0.42	±5
κ_1 +	-0.05	±5
Cp_{01} *	51.89	±15 [23]
Cp_{02} *	741.34	±15 [23]
Cp_{03} *	-416.10	±15 [23]
Cp_{04} *	70.00	±15 [23]
Boundary Conditions (BC)		
T_0 / °C+	252.00	±0.2
P_0 / bar+	18.40	±0.5

* Experimental + Assumed

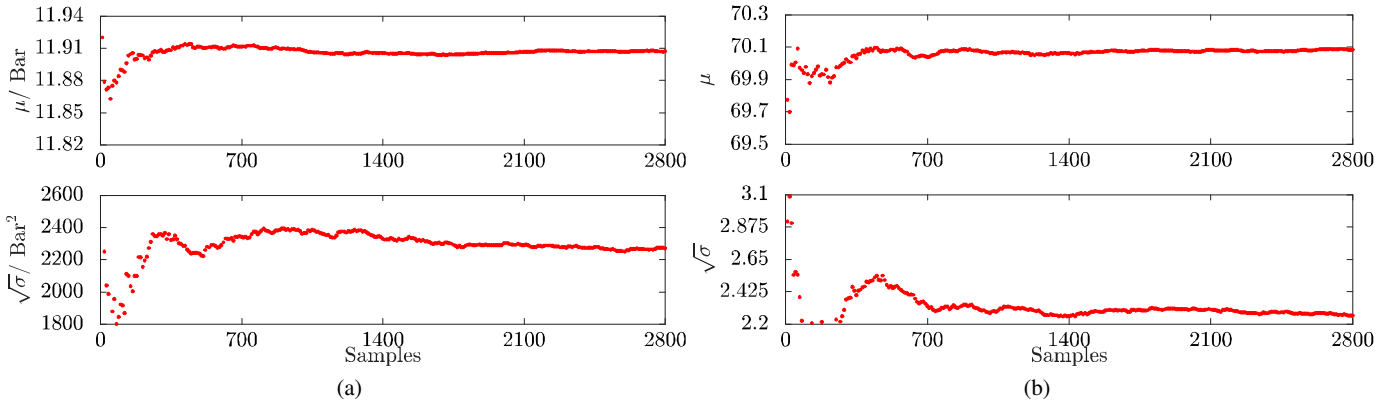

Fig. 3: (a) Convergence plots of the first and second order moments for the static pressure at the throat. (b) Convergence plots of the first and second order moments for $\theta = 26.25\,^{\circ}$ at $x = 3.1$mm from the throat.

determined locations on the nozzle centerline and then solving the jump conditions for an arbitrary turning angle of the obstacle [20].

Fig. 2 summarizes the workflow of the overall calculation method to propagate the uncertainties of the model closure coefficients and of the boundary conditions (BCs) through the CFD and the steady shock wave solver. The uncertainty of the input parameters are propagated through the numerical model via a Monte Carlo (MC) method [21]. The MC method is initialized with 2500 samples distributed within the design space through a Latin Hypercube method. Fig. 3a and Fig. 3b show the convergence results for two SRQs which required the largest number of samples to converge.

4.1. Model Uncertainties

Two sources of model uncertainties are considered in this study. The first are related to the closure parameters of the iPRSV EoS [24], which is a commonly selected EoS because it offers a sufficient balance between computational cost and accuracy [25]. The properties attributed to MM have been tabulated in Tab. 1 with the assumed values and the associated uncertainty [23]. A study conducted by Iyer [26] pointed out that the acentric factor and κ term have negligible influence on the SRQs for the operating conditions of interest. The second source of uncertainty originates from fluctuations in the stagnation BCs reported in Tab. 1. The probability density function of the uncertain parameters is assumed to be uniform due to the limited data available, resulting in a U_{input}, as defined in Eqn. 1

and shown in Fig. 4 and 6a for β and static pressure with a 95 % confidence level, respectively. Note that the only deterministic value considered is the static nozzle back pressure, fixed at 2.1 bar.

As already mentioned, the most important contribution to U_{num} is the discretization error. To assess this contribution, a grid convergence study based on the procedure given in Ref. [14,17] was performed. The outcomes showed that an unstructured mesh of 10000 elements provides mesh independence results and, as such, that U_{num} can be deemed negligible compared to U_{input}. Thus, it will not be taken into account in the following analysis.

4.2. Experimental Uncertainties

A numerical model similar to the one described above was used to replicate the actual experiments. This is referred to as pseudo-experiment in the following. Unlike the iPRSV, the multi-parameter Span-Wagner model [27] was adopted to characterize the thermodynamic properties of the fluid. Two types of experimental uncertainties were considered, namely the uncertainties due to the fluctuations in the BCs and the uncertainties related to the measurement technique utilized in the experiments. The former type is formally termed as Type A according to [28,29]. Conversely, the latter type, formally referred to as Type B uncertainties, originates from the measurement chain and are commonly identified from wind tunnel calibration procedures [30–32].

With reference to the value of β, there are three predominant factors that may contribute to errors in the measurements; namely, boundary layer effects on the wedge, uncertainties in the wedge model manufacturing and alignment, and errors in measuring the flow direction. According to the analytical studies of [31], the boundary layer, which affects the flow turning angle θ, causes an angular flow deviation U_{BL} of 0.25° in β. In absence of any further information regarding the associated probability density function, this value is assumed to be uniformly distributed. The manufacturing uncertainties U_{DF} related to the wedge model were quantified by Molder [31] to be equal to ± 0.1 °. Next, the uncertainty due to the model alignment U_{FA} was estimated by the same author to be equal to ± 1 °.

As far as the static pressures measurements are concerned, the uncertainty U_{SP}, assumed to be uniformly distributed, is dependent on the accuracy of the adopted measuring device. The Scanivalve DSA3217 Digital Sensor Array (DSA) [33] was chosen. It is a stand-alone electronic pressure scanner with an accuracy equal to 0.05 % of the full scale, which varies along the expansion path.

Provided that the uncertainties are statistically independent, the overall uncertainty related to the measured values of β and static pressure can be computed by quadrature summation, once the uniform distributions have been transformed into equivalent Gaussian using the procedure recommended in Ref. [28]. Eventually, the overall uncertainties are given by $U_{\text{c:}\beta} = \sqrt{{U_{\text{BC}}}^2 + U_{\text{BL}}^2 + U_{\text{DF}}^2 + U_{\text{FA}}^2}$, and $U_{\text{c:}p} = \sqrt{{U_{\text{BC}}}^2 + U_{\text{SP}}^2}$, respectively. The uncertainty related to a 95% confidence level is given by a final U_{D}, see Eqn. 1, which is equal to $2U_{\text{c}}$ [28,29].

5. Results and Discussion

Figure 5 shows the validation comparison error $|E|$ and the validation standard uncertainty U_{val} of β as a function of θ, calculated with Eqn. 1 and 2, respectively. The results displayed refer to two different nozzle locations, one close to the throat and the other one close to the nozzle exit. In both cases, the validation comparison error $|E|$ is less than the validation uncertainty U_{val}. According to the validation method discussed in Sect. 2, this means that the model predicts the shock wave angle adequately at all sampled flow turning angles θ. Interestingly, the validation standard uncertainty U_{val} is larger for predicted β values close to the throat. Such a trend indicates that the input uncertainties, which are propagated through the model, have a more pronounced effect on the SRQs in regions in which the flow is highly non-ideal.

It is also worth noticing that the difference $U_{\text{val}} - |E|$ is larger for β values predicted close to the throat. Together with a smaller $|E|$, this may erroneously suggest that the model predictions are more accurate than those at the nozzle exit. To illustrate this, the magnitude of the model uncertainty band is compared in Fig. 4 with the one associated to the measurements. More specifically, Fig. 4 shows the relation between the shock wave angle β and the flow turning angle θ – i.e., the semi-aperture angle – for a wedge inserted in the flow. The uncertainty bars resulting from the calculation method are superimposed to the averaged values of both the model prediction and pseudo-measurements. The curves indicated correspond to the chosen physical distances from the throat. The relative contribution of U_{input}, i.e. the uncertainties associated to model parameters, compared to U_{D} (see Eqn. 1), i.e. those relative to the experiment, is approximately between 2 and 5 times larger, depending on the considered location along the nozzle.

These results highlight that the model predictions are more uncertain in the regions where the flow non-ideality is more prominent. The thermo-physical submodel has an arguable margin of improvement although it can be deemed validated according to the metrics. This information is missing in the comparison between U_{val} and $|E|$, which must

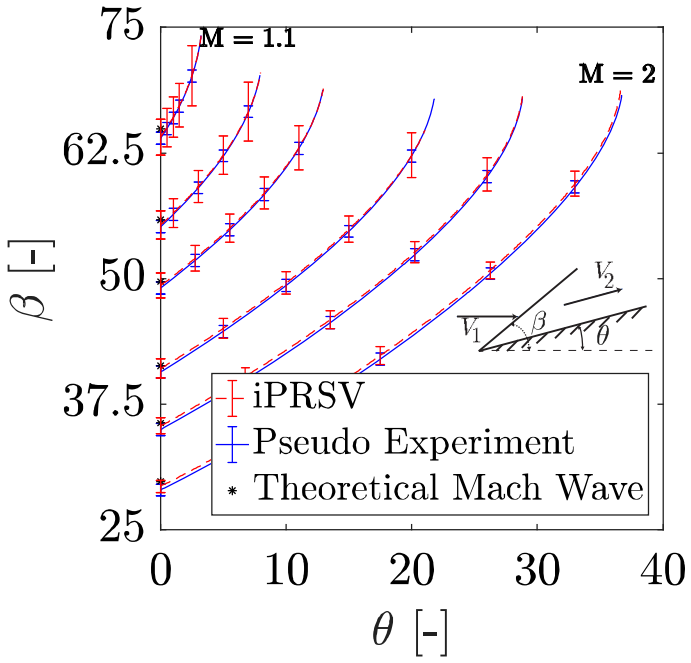

Fig. 4: The $\theta-\beta-M$ diagram with model and measurement uncertainties. Incremented distances from the throat 3.1 mm (M = 1.1), 5.9 mm (M = 1.2), 8.8 mm (M = 1.3), 14.7 mm (M = 1.5), 21.4 mm (M = 1.7) and 56 mm (M = 2) predicted with the iPRSV EoS, see Fig. 1b.

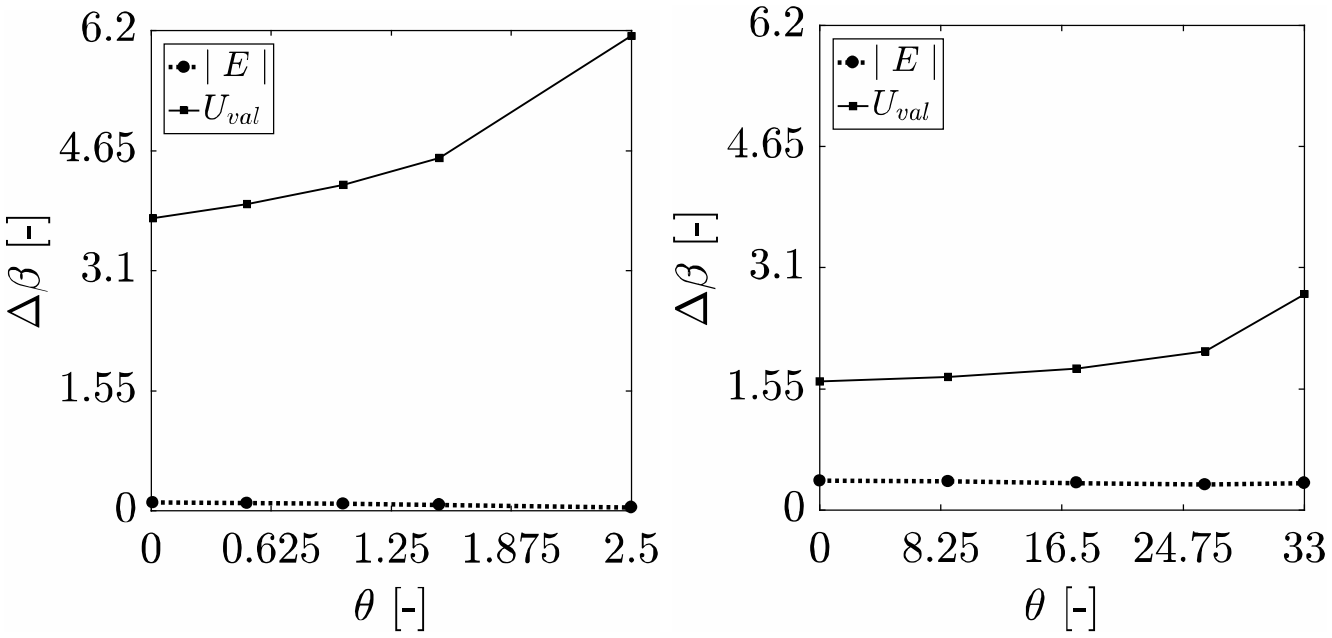

(a) (b)

Fig. 5: The comparison and validation metrics of the shock-wave angles for: (a) M = 1.1 (close to throat); (b) M = 2 (close to exit).

be then complemented by additional statistical indicators taking into account the extent of the uncertainty bands associated with the model predictions and the experimental value.

Similar conclusions can be inferred by looking at the variation of the model uncertainties with the Mach number. At a given Mach number, the model uncertainty gradually increases while approaching the detachment point, see Fig. 4. Finally, it is important to note that U_{D} remains approximately constant because the contributions from the Type A uncertainties, i.e., the BCs, are negligible compared to the Type B, which are indeed assumed constant in this validation exercise.

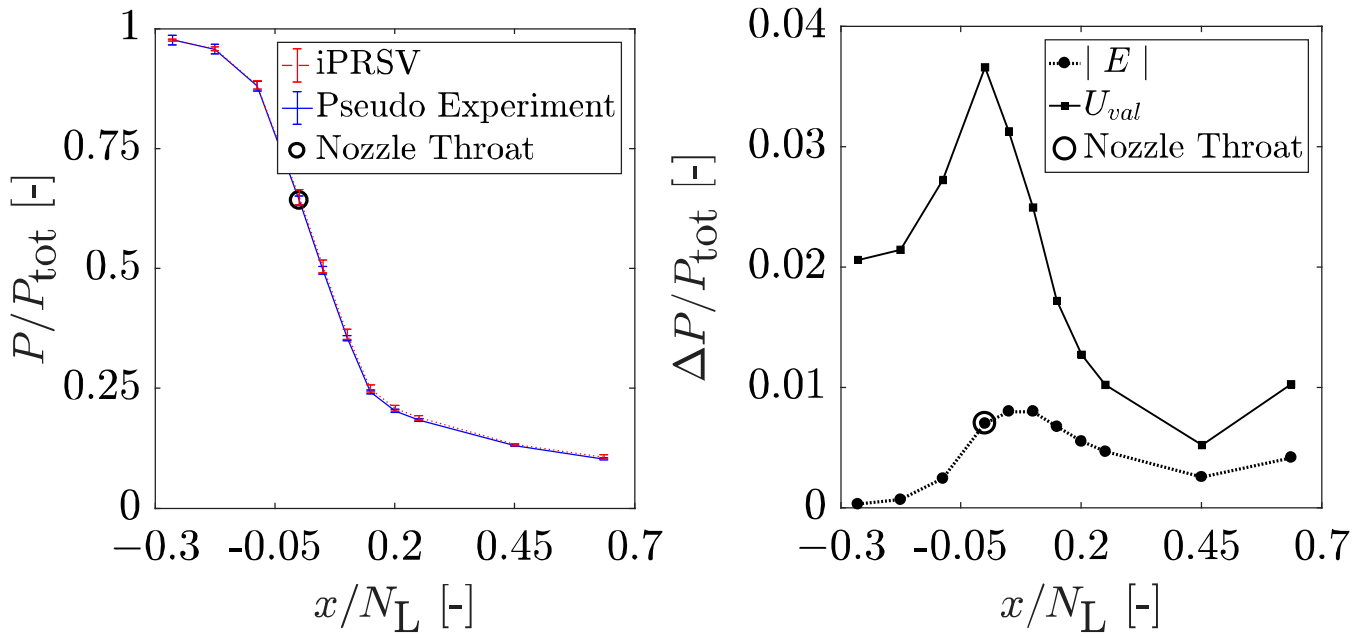

Fig. 6: a) The variation in static pressure together with the uncertainty bands in the model and experiment. b) The comparison validation metrics for static pressure vs. non-dimensional distance along the expansion path. Eleven coordinates correspond to the individual pressure taps.

Figure 6a shows the dimensionless static pressure along the nozzle for the second envisaged experiment. P_{tot} is the inlet total pressure and N_{L} is the nozzle length for both the pseudo experiment and model predictions. Figure 6b shows the validation metrics $|E|$ and U_{val} expressed in terms of dimensionless static pressure. Similarly to the shock wave angle predictions, the accuracy of the model results for the static pressure is dependent on the location inside the nozzle, as exemplified by the varying $|E|$ and the difference $|E|$ - U_{val}. The highest discrepancy occurs at the throat, while approaching the nozzle exit the comparison error $|E|$ and U_{val} gradually decrease. Surprisingly, the model and the pseudo experiment are in the closest agreement at the inlet. Moreover, in contrast with what is observed for β predictions, the error band associated to model results is comparable in magnitude or even smaller than that expected for the measurements. This suggests that the static pressures values estimated by the model are less sensitive to uncertainties in the EoS closure parameters, or the accuracy in the measurement chain is lower than that involved in measuring the shock angles. The first experiment is, then, arguably more suited to assess the model validity where non-ideal gas effects are more prominent.

6. Conclusions

In this paper, a validation exercise has been performed to show how the predictive capability of the thermodynamic model of a NICFD solver can be assessed against experimental data. To this end, a numerical procedure based on uncertainty quantification analysis has been conceived to compare the model predictions with experiments. The outcomes of the study demonstrate the applicability of the procedure, provided that the assumed ranges of model and experimental uncertainties hold. Furthermore, it can be argued that the method can benefit from the introduction of additional statistical indicators taking explicitly into account the model uncertainty band. Ongoing work will focus on this aspect and on the extension of the approach to the validation of the turbulence submodels.

Acknowledgements

The research work was conducted in the framework of two research programs on mini-ORC systems funded by the Dutch Technology Foundation STW and the partners Dana Belgium NV and Robert Bosch GmbH (grant numbers 12811 and 13385). The authors would also like to express their gratitude to Richard Dwight for his suggestions concerning code validation.

References

[1] Casati, E., Vitale, S., Pini, M., Persico, G., Colonna, P.. Centrifugal turbines for mini-Organic Rankine cycle power systems. *J Eng Gas Turb Power* 2014;136(12):122607.

[2] Guardone, A., Spinelli, A., Dossena, V.. Influence of molecular complexity on nozzle design for an organic vapor wind tunnel. *J Eng Gas Turb Power* 2013;.

[3] Head, A., De Servi, C., Casati, E., Pini, M., Colonna, P.. Preliminary design of the ORCHID: A facility for studying non-ideal compressible fluid dynamics and testing ORC expanders. In: ASME Turbo Expo. GT2016-56103; 2016, p. 14.

[4] Economon, T.D., Palacios, F., Copeland, S.R., Lukaczyk, T.W., Alonso, J.J.. SU2: An open-source suite for multiphysics simulation and design. *AIAA Journal* 2015;54(3):828–846.

[5] Vitale, S., Gori, G., Pini, M., Guardone, A., Economon, T.D., Palacios, F., et al. Extension of the SU2 open source CFD code to the simulation of turbulent flows of fuids modelled with complex thermophysical laws. In: Proceedings of the 22nd AIAA computational fluid dynamics conference. American Institute of Aeronautics and Astronautics; 2015, p. 1–12.

[6] Reinker, F., Hasselmann, K., aus der Wiesche, S., Kenig, E.Y.. Thermodynamics and fluid mechanics of a closed blade cascade wind tunnel for organic vapors. *J Eng Gas Turbines Power* 2015;138(5):052601.

[7] Spinelli, A., Pini, M., Dossena, V., Gaetani, P., Casella, F.. Design, Simulation, and Construction of a Test Rig for Organic Vapors. *J Eng Gas Turb Power - T ASME* 2013;135(4):10.

[8] Spinelli, A., Cozzi, F., Dossena, V., Gaetani, P., Zocca, M., Guardone, A.. Experimental investigation of a non-ideal expansion flow of siloxane vapor MDM. 2016.

[9] Oberkampf, W.L., Trucano, T.G.. Verification and validation in computational fluid dynamics. *Prog in Aerosp Sciences* 2002;38(3):209 – 272.

[10] Roache, P.J.. Fundamentals of verification and validation. Hermosa publ.; 2009.

[11] Oberkampf, W.L., Roy, C.J.. Verification and Validation in Scientific Computing. Cambridge University Press; 2010.

[12] Roy, C., Oberkampf, W.. A complete framework for verification, validation, and uncertainty quantification in scientific computing (invited). In: Aerospace Sciences Meetings. AIAA; 2010, p. 124.

[13] Guide for the Verification and Validation of Computational Fluid Dynamics Simulations. AIAA; 1998.

[14] Standard for Verification and Validation in Computational Fluid Dynamics and Heat Transfer. ASME V&V 20; 2009.

[15] Coleman, H.W., Stern, F.. Uncertainties and CFD code validation. *J of Fluids Engg* 1997;119(4):795–803.

[16] Eca, L., Vaz, G., Hoekstra, M.. Code verification, solution verification and validation in RANS solvers. In: ASME 2010 29th International Conference on Ocean, Offshore and Arctic Engineering. 49149; 2010, p. 597–605.

[17] Celik, I.B., Ghia, U., Roache, P.J., Freitas, C.J., Coleman, H., Raad, P.E.. Procedure for estimation and reporting of uncertainty due to discretization in CFD applications. *J of Fluids Engg* 2008;130(7).

[18] Hill, J., Baron, J., Schindel, L., Markham, J.. Mach number measurements in high-speed wind tunnels. Tech. Rep.; NATO; 1956.

[19] Schueler, C.J.. An investigation of the model blockage for wind tunnels at mach numbers 1.5 to 19.5. Tech. Rep.; Arnold Engineering Development Center; 1960.

[20] Grossman, B.. Fundamental concepts of real gasdynamics. Tech. Rep.; Virginia Tech; 2000.

[21] Adams, B., Bauman, L., Bohnhoff, W., Dalbey, K., Ebeida, M., Eddy, J., et al. Dakota, a multilevel parallel object-oriented framework for design optimization, parameter estimation, uncertainty quantification, and sensitivity analysis: Version 6.0 user manual. Tech. Rep.; Sandia Labs.; 2014.

[22] Rowley, R., Wilding, W., Oscarson, J., Yang, Y., Zundel, N., Daubert, T., et al. DIPPR Data compilation of pure chemical properties. Design Institute for Physical Properties, AIChE, New York, NY; 2004.

[23] Colonna, P., Nannan, N.R., Guardone, A., Lemmon, E.W.. Multiparameter equations of state for selected siloxanes. Fluid Phase Equilib 2006;244:193–211.

[24] van der Stelt, T., Nannan, N.R., Colonna, P.. The iPRSV equation of state. *Fluid Phase Equilib* 2012;330:24–35.

[25] Cinnella, P., Congedo, P., Pediroda, V., Parussini, L.. Sensitivity analysis of dense gas flow simulations to thermodynamic uncertainties. *Phys Fluids* 2011;23(11):116101.

[26] Iyer, S.. Influence of thermodynamic property perturbations on nozzle design and non-ideal compressible flow phenomena. Master's thesis; Delft University of Technology; 2015.

[27] Lemmon, E., Huber, M., McLinden, M.. NIST standard reference database 23: Reference fluid thermodynamic and transport properties-REFPROP, version 9.1,. Tech. Rep.; National Institute of Standards and Technology, Standard Reference Data Program, Gaithersburg; 2013.

[28] Measurement uncertainty analysis principles and methods. Tech. Rep.; National Aeronautics and Space Administration; 2010.

[29] Test Uncertainties. ASME PTC 19.1; 2013.

[30] Culberison, P.. Calibration report on the university of michigan supersonic wind tunnel. Tech. Rep.; ARC - University of Michigan; 1949.

[31] Molder, S.. Head-on interaction of oblique shock waves. Tech. Rep.; University of Toronto; 1960.

[32] Norris, J.D., Pierpont, P.K.. Experimental performance of a conical pressure probe at mach numbers of 3.0, 4.5, and 6.0. Tech. Rep.; Langley Reseurch Center; 1966.

[33] Digital sensor array: DSA 3007, 3207, 3307 Series modules, Instruction and service manual. Scanivalve Corp.; 2016.